



Discovery of 5-substituted-*N*-arylpyridazinones as inhibitors of p38 MAP kinase

Kevin D. Jerome*, Michael E. Hepperle[†], John K. Walker, Li Xing, Rajesh V. Devraj, Alan G. Benson[‡], John E. Baldus, Shaun R. Selness

Pfizer Global Research and Development, St. Louis Laboratories, 700 Chesterfield Pkwy. W., Chesterfield, MO 63017, USA

ARTICLE INFO

Article history:

Received 28 January 2010

Revised 24 March 2010

Accepted 26 March 2010

Available online 31 March 2010

Keywords:

p38
Pyridazinones
Kinase

ABSTRACT

The synthesis, structure–activity relationship and modeling of a series of 5-substituted-*N*-aryl pyridazinone based p38 α inhibitors are described. In comparing the series to the similar *N*-aryl pyridinone series, it was found that the pyridazinones maintained a weaker interaction to the p38 enzyme, and therefore showed generally weaker binding than the pyridinones.

© 2010 Elsevier Ltd. All rights reserved.

Inhibition of the p38 α mitogen-activated protein (MAP) kinase has been the focus of much pharmaceutical and academic research in recent years.¹ p38 has been pursued as a kinase target for such diseases as rheumatoid arthritis (RA), Crohn's disease, inflammatory bowel syndrome (IBS), and psoriasis.² p38 is a serine/threonine dual specificity kinase that has four known isoforms (α , β , γ , and δ), with their expression varying among cell types of the immune system. p38 α is the chief isoform implicated in inflammatory disease.³

One current treatment option for these inflammatory diseases is with biological agents known for successfully shutting down tumor necrosis factor α (TNF- α function.⁴ Preclinical studies strongly support that selective inhibition of p38 α can effectively modulate TNF- α , as well as interleukin-1 β (IL-1 β) and other cytokine production. Because TNF α and IL-1 β have been implicated as key cytokines in inflammatory diseases, it is anticipated that a small molecule p38 α MAP kinase inhibitor should provide therapeutic value for the treatment of such inflammatory conditions.

Some historical p38 inhibitors are shown in Figure 1. Researchers at Vertex have previously demonstrated both potency and selectivity versus p38 α kinase with inhibitors such as VX-745, **1**.⁵ More recently, Merck reported a series of potent 6-imidazopyridinyl-2-arylpyridazin-3-one p38 inhibitors **2**,⁶ followed by a series of 6-arylamino-2-arylpyridazin-3-ones **3**⁷ that also showed good p38 α potency and selectivity versus p38 γ , p38 δ , JNKs and ERKs.

* Corresponding author. Tel.: +1 636 247 8655; fax: +1 636 247 0966.

E-mail address: jerome52@sbcglobal.net (K.D. Jerome).

[†] Present address: Nycomed GmbH, Byk-Gulden-Str. 2/F21.311, D-78467 Konstanz, Germany.

[‡] Present address: Pharmaceutical Products, Covidien, 675 McDonnell Blvd., Hazelwood, MO 63042, USA.

We herein describe the discovery of a series of 5-substituted-*N*-aryl pyridazinones as potent p38 inhibitors, derived from the *N*-benzyl pyridinone high-throughput screening hit, SC-25028, **4**. The evolution of the pyridinone template is shown in Figure 2. The enzyme activity of **4** against p38 α was modest at 0.68 μ M. However, evaluation of **4** against a panel of 48 kinases revealed that the compound was selective for p38 (less than 30% inhibition at 10 μ M against the entire panel). Metabolic stability of **4** was recognized as the primary liability as revealed by its incubation with human liver microsomes (52% parent remaining after 45 min of incubation). Previous reports have shown optimizations of **4** in the pyridinone template to develop *N*-benzyl inhibitors⁸ such as **5**. Further optimization of this template led to *N*-aryl pyridinone inhibitors, culminating in the clinical candidate PHA-797804,⁹ **6**.

In conjunction with our efforts in the *N*-aryl pyridinone scaffold, we initiated the investigation of *N*-aryl pyridazinones as p38 α inhibitors (Fig. 3), based on the similarity in structural overlay and similar presentation of suitable binding motifs. In addition to

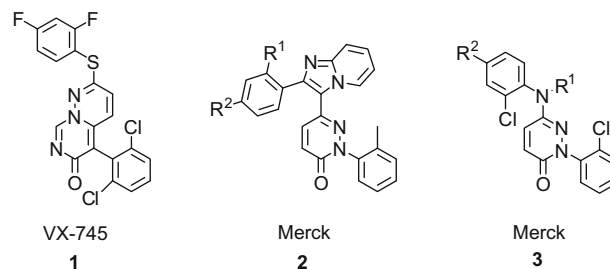


Figure 1. Historical p38 inhibitors.

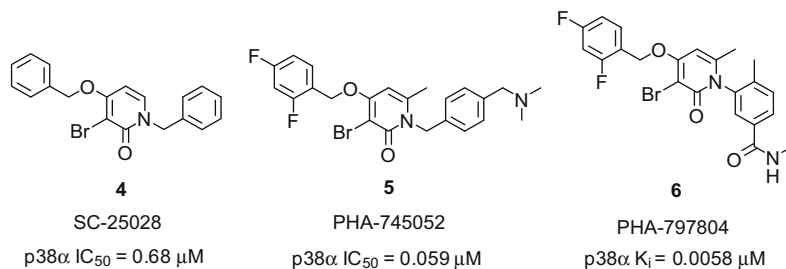


Figure 2. Pyridinone p38 α inhibitors based on SC-25028.

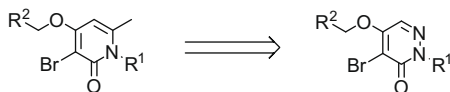


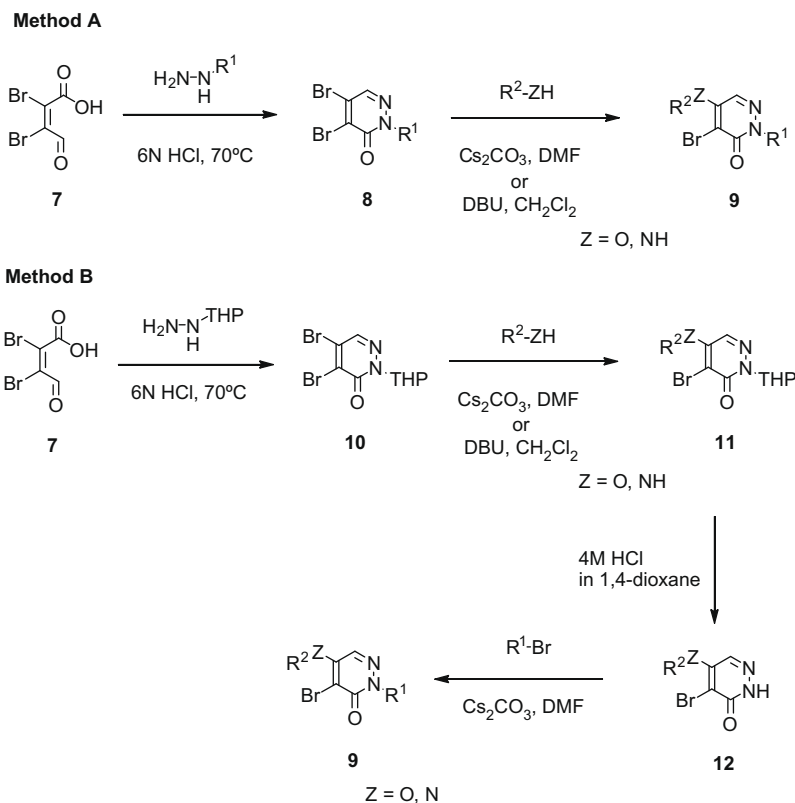
Figure 3. Structure Based Drug Design of *N*-aryl pyridazinones from *N*-aryl pyridinones.

extending our intellectual property position, we also anticipated a reduction in log *P* with the pyridazinones, which was expected to increase inherent solubility of the series. Using the pyridazinone core also removes the C-6 methyl of the pyridinone core and the accompanying chirality due to stable atropisomers formed by the aryl pyridinone analogs,⁹ such as **6**, which is the single aS atropisomer. Initial analogs were based on the initial lead **4** and the SAR gleaned from the development of **5**.

Two generalized syntheses of the pyridazinone template are shown in Scheme 1.¹⁰ Method A allows for the diversification of the C-5 position with a fixed N-2, and method B allows for the diversification of the N-2 position, with a fixed C-5. In method A, mucobromic acid **7** was condensed with hydrazines in 6 N HCl at

70 °C to form an N-2 substituted, 4,5-dibromo pyridazinone **8**.¹¹ Nucleophiles were then used to displace the C-5 bromide to form **9**. For amines, Cs₂CO₃ in DMF were the standard conditions. For alcohols, either Cs₂CO₃ in DMF or DBU in methylene chloride could be used. This displacement occurred exclusively at C-5, leaving the C-4 bromide intact.¹² In method B, **7** was condensed with THP hydrazine to form the N-2 THP, 4,5-dibromo pyridazinone **10**. A similar nucleophile displacement to that described above formed **11**. Deprotection, followed by reaction with alkyl and aryl bromides gave **9**.

Initially, we investigated pyridazinone mimics of the screening hit **4**. The direct pyridazinone mimic **13**, where Z = O and R¹, R² = benzyl, was found to be inactive against p38 α (Table 1). Modifying the R¹ group to a phenyl **14** gave modest activity. Modification of R² to a 2,4-difluorobenzoyloxy **15**, which was known to be an optimal group in the *N*-aryl pyridinone series, showed a 10-fold increase in potency to 2.7 μ M against p38 α . Another dramatic increase in potency was seen when R¹ was replaced with 2,6-dichlorophenyl, as found in **1**, which is known to impart a desired orthogonality to the R¹ phenyl ring.



Scheme 1. Alternate syntheses of the pyridazinone scaffold.

Table 1
p38 α Potency of selected 4-bromo-disubstituted pyridazinones

Compd	Method	Z	R ¹	R ²	p38 α ^a IC ₅₀ (μ M)
13	A	O	Benzyl	Benzyl	>100
14	A	O	Phenyl	Benzyl	24.4
15	A	O	Phenyl	2,4-DiF bz	2.70
16	A	O	2,6-DiClPh	Benzyl	1.39
17	A	N	2,6-DiClPh	Benzyl	5.72
18	A	O	2,6-DiClPh	Phenethyl	3.14
19	A	N	2,6-DiClPh	Phenethyl	3.81
20	A	O	2,6-DiClPh	4-F bz	1.32
21	A	N	2,6-DiClPh	4-F bz	12.3
22	A	O	2,6-DiClPh	2,4-DiF bz	0.16
23	A	O	2,6-DiClPh	2,4,6-TriF bz	0.54
24	A	O	2,6-DiClPh	3,4-DiF bz	2.07
25	A	O	2,6-DiClPh	2,3,4-TriF bz	0.47
26	A	O	2,6-DiClPh	2-F-4-ClPh	1.01
27	B	O	2,6-DiCl-4-pyr	2,4-DiF bz	0.25
28	B	O	2,6-DiFPh	2,4-DiF bz	0.59

^a All analogs were >200 μ M versus JNK2.

With a suitable R¹ group in place, the focus was shifted to further optimization of R². As analogs **16–26** show, 2,4-difluorobenzyloxy was found to be optimal in the pyridazinone series as well, with **22** showing 160 nM inhibition of p38 α . Compounds **17**, **19** and **21** were prepared to evaluate the role of the C-5 linkage. In all cases, this change showed a decrease in p38 α inhibition.

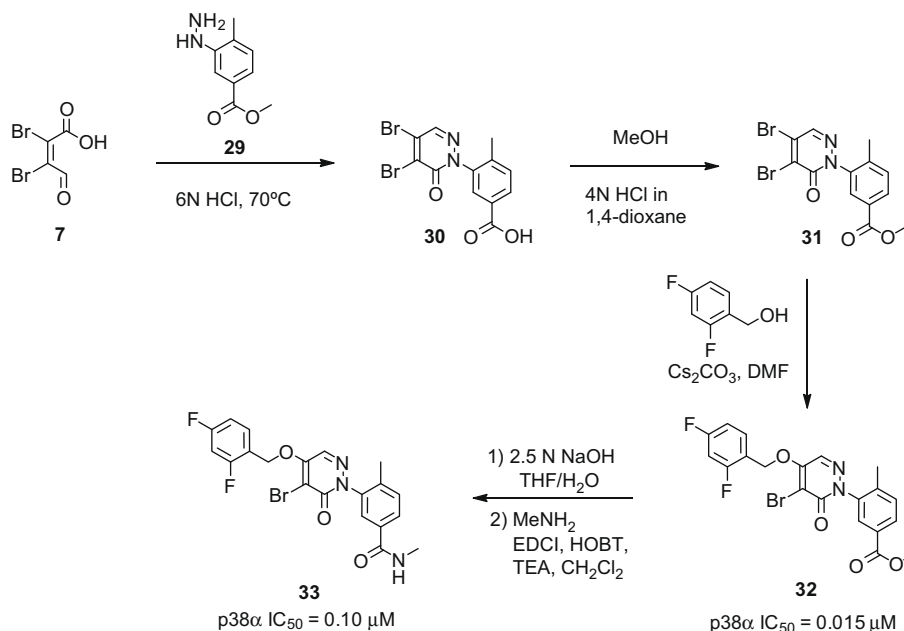
Further optimization was attempted at R¹, as shown in **27** and **28**, but failed to improve potency.

In an attempt to minimize the molecular weight of the analogs and thereby increase the inherent solubility of the series, changes were made at C-4 in an attempt to discover a suitable Br replacement. This group at C-4 occupies a shallow lipophilic pocket adjacent to the deep hydrophobic selectivity pocket as defined by Thr106. This group also favors proper orientation about the ether linkage to optimize the benzyloxy group's interaction with the selectivity pocket. The optimal C-4 group would be big enough to cause the C-5 benzyl group to swing into the critical hydrophobic selectivity pocket, yet small enough to still fit into its own shallow lipophilic pocket. Despite synthesizing several analogs with alternate C-4 substituents, such as Me, Cl and I, Br was found to be optimal.

Based on SAR gleaned from the *N*-aryl pyridinone series, the corresponding analog to the clinical candidate **6** was synthesized in the pyridazinone series (Scheme 2). The synthesis of **32** preceded by method A, as shown in Scheme 1. The methyl ester of **32** was hydrolyzed and **33** was then formed via an amide bond coupling with methylamine. Compounds **32** and **33** were both active against p38 α , with **32** showing an order of magnitude increase in potency over **22**.

Based on modeling, the binding of pyridazinone compounds are consistent with that of the pyridinone series. Compound **32** was docked into the p38 α binding pocket using AGDOCK (Fig. 4).¹³ The protein model is derived from the **6**-p38 α binary complex,⁹ with 2A cushions in each dimension of the docking box and a maximum energy barrier of 25 kcal/mol. Consistent with the pyridinone binding, the 2,4-difluorobenzyloxy moiety of **32** occupies the unique p38 encapsulated hydrophobic pocket, defined by Thr106 as the gate keeping residue. The pyridazinone carbonyl forms bifurcated hydrogen bonds with the kinase hinge, in which Gly110 undergoes a peptide flip that is prohibited by other amino acids bearing a side chain. The orientation of the *N*-methyl benzamide of **6** is designated by the polar interaction of the amide NH and the backbone of Gly110. However, modeling of **32** suggests that the hydrophobic contact between the methyl amide and the side chain of Leu108 (~4 Å) disrupts the binding conformation. In particular the sevenfold activity loss of the *N*-methyl amide analog **33** over the methyl ester **32** appears to support this binding model.

In general, the pyridazinone series was found to be less potent than the pyridinone series. Since orthogonality between the *N*-aryl and the core is required by target binding, the removal of the 6-methyl when comparing the pyridinone template to the pyridazinone introduces conformational entropy loss from the free-ligand state to the bound state for the pyridazinone series. Also, the electronic properties of the pyridazinone carbonyl oxygen, the acceptor of the critical bifurcated hydrogen bond, are influenced by the atomic composition of the aryl ring. Density functional theory (DFT) calculations performed on the cores reveal that the electrostatic potential (ESP) charge of the oxygen atom decreases from -0.50 for pyridazinone to -0.56 for pyridinone, a factor of 12%.¹⁴



Scheme 2. Synthesis of the pyridazinone analog of **6**.

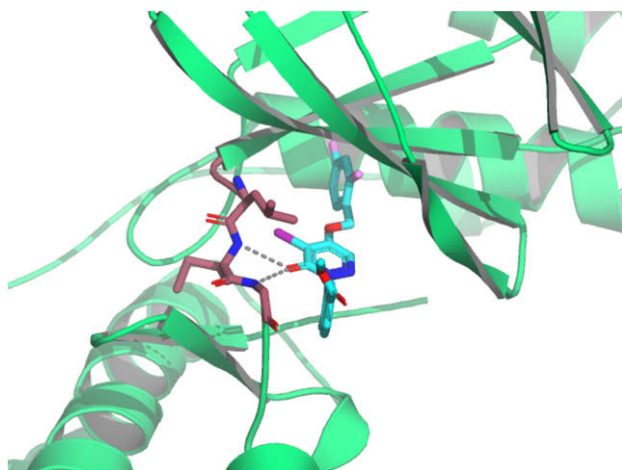


Figure 4. Pyridazinone **32** modeled into the p38 α binding pocket.

Hence, the carbonyl of the pyridinone core is a better hydrogen bond acceptor than the carbonyl of the pyridazinone core, giving rise to a more favorable hydrogen bond interaction with the p38 enzyme.

In summary, a series of 5-substituted-*N*-aryl pyridazinones were synthesized and found to be respectable p38 α inhibitors. However, when compared to *N*-aryl pyridinone inhibitors such as **6**, it was found that the pyridazinones maintained a weaker bifurcated hydrogen bond interaction to the p38 enzyme, as well as a decreased ability to maintain orthogonality between the *N*-aryl group and the pyridazinone core, both of which led to generally weaker p38 α enzyme activity in the pyridazinone series versus the pyridinone series.

References and notes

- Dominguez, C.; Tamayo, N.; Zhang, D. *Expert Opin. Ther. Pat.* **2005**, *15*, 801.
- (a) Arend, W. P.; Dayer, J. M. *Arthritis Rheum.* **1990**, *33*, 305; (b) Firestein, G. S.; Alvaro-Gracia, J. M.; Maki, R. J. *Immunol.* **1990**, *144*, 3347; (c) Rutgeerts, P.; D'Haens, G.; Targan, S.; Vasilias, E.; Hanauer, S. B.; Present, D. H.; Mayer, L.; Van Hogeand, R. A.; Braakman, T.; DeWoody, K. L.; Shaible, T. F.; Van Deventer, S. J. *Gastroenterology* **1999**, *117*, 761; (d) Ulfgren, A. K.; Andersson, U.; Engstrom, M.; Klareskog, L.; Maini, R. N.; Taylor, P. C. *Arthritis Rheum.* **2000**, *43*, 2391.
- (a) Foster, M. L.; Halley, F.; Souness, J. E. *Drug News Perspect.* **2000**, *13*, 488; (b) Lee, J. C.; Laydon, J. T.; McDonnell, P. C.; Gallagher, T. F.; Kumar, S.; Green, D.; McNulty, D.; Blumenthal, M. J.; Heys, J. R.; Landvatter, S. W.; Strickler, J. E.; McLaughlin, M. M.; Siemens, I. R.; Fisher, S. M.; Livi, G. P.; White, J. R.; Adams, J. L.; Young, P. R. *Nature* **1994**, *372*, 739.
- Enbrel is a marketed soluble TNF- α receptor and Remicade is marketed as a TNF- α antibody therapy: (a) Jarvis, B.; Faulds, D. *Drugs* **1999**, *57*, 945; (b) Rutgeerts, P. J. *Aliment. Pharmacol. Ther.* **1999**, *13*, 9; (c) Seymour, H. E.; Worsley, A.; Smith, J. M.; Thomas, S. H. L. *Br. J. Clin. Pharmacol.* **2001**, *51*, 201; For other clinical examples of p-38 map kinase inhibitors efficacy see: Ferraccioli, G. F. *Curr. Opin. Anti-Inflamm. Immunomodulat. Invest. Drugs* **2000**, *2*, 74.
- (a) Bemis, G. W.; Salituro, F. G.; Duffy, J. P.; Cochran, J. E.; Harrington, E. M.; Murcko, M. A.; Wilson, K. P.; Su, M.; Galullo, V. P. U.S. Patent 7,365,072 **B2**, 2008.; (b) Bemis, G. W.; Salituro, F. G.; Duffy, J. P.; Harrington, E. M. U.S. Patent 6,147,080, 2000.
- Colletti, S. L.; Frie, J. L.; Dixon, E. C.; Singh, S. B.; Choi, B. K.; Scapin, G.; Fitzgerald, C. E.; Kumar, S.; Nichols, E. A.; O'Keefe, S. J.; O'Neill, E. A.; Porter, G.; Samuel, K.; Schmatz, D. M.; Schwartz, C. D.; Shoop, W. L.; Thompson, C. M.; Thompson, J. E.; Wang, R.; Woods, A.; Zaller, D. M.; Doherty, J. B. *J. Med. Chem.* **2003**, *46*, 349.
- Natarajan, S. R.; Heller, S. T.; Nam, K.; Singh, S. B.; Scapin, G.; Patel, S.; Thompson, J. E.; Fitzgerald, C. E.; O'Keefe, S. J. *Bioorg. Med. Chem. Lett.* **2006**, *16*, 5809.
- Selness, S. R.; Devraj, R. V.; Monahan, J. B.; Boehm, T. L.; Walker, J. K.; Devadas, B.; Durlay, R. C.; Kurumbail, R.; Shieh, H.; Xing, L.; Hepperle, M.; Jerome, K. D.; Benson, A. G.; Marrufo, L. D.; Madsen, H. M.; Hitchcock, J.; Owen, T. J.; Christie, L.; Promo, M. A.; Hickory, B. S.; Alvira, E.; Naing, W.; Bleviss-Bal, R. *Bioorg. Med. Chem. Lett.* **2009**, *19*, 5851.
- Xing, L.; Shieh, H. S.; Selness, S. R.; Devraj, R. V.; Walker, J. K.; Devadas, B.; Hope, H. R.; Compton, R. P.; Schindler, J. F.; Hirsch, J. L.; Benson, A. G.; Kurumbail, R. G.; Stegeman, R. A.; Williams, J. M.; Broadus, R. M.; Walden, Z.; Monahan, J. B. *Biochemistry* **2009**, *48*, 6402.
- Full disclosure of chemistry methods is made in the following patent application: Devraj, R.; Hepperle, M.; Jerome, K.; Selness, S.; Walker, J. K. PCT Int. Appl. 2005, 169 pp. WO 2005007632.
- (a) Santagati, N. A.; Duro, F.; Caruso, A.; Trombadore, S.; Amico-Roxas, M. *Farmaco, Ediz. Sci.* **1985**, *40*, 921; (b) Gudriniece, E.; Karklins, A. *Latv. PSR Zinat. Akad. Vestis Kim. Ser.* **1967**, *4*, 474; (c) Bourdais, S. *Bull. Soc. Chim. Fr.* **1964**, 2124.
- (a) Matyus, P.; Czako, K.; Behr, A.; Varga, I.; Podanyi, B.; Von Arnim, M.; Varkonyi, P. *Heterocycles* **1993**, *36*, 785; (b) Gomez-Gil, M. C.; Gomez-Parra, V.; Sanchez, F.; Torres, T. *Liebigs Ann. Chem.* **1985**, 1465.
- Verkhivker, G. M.; Bouzida, D.; Gehlhaar, D. K.; Rejto, P. A.; Arthurs, S.; Colson, A. B.; Freer, S. T.; Larson, V.; Luty, B. A.; Marrone, T.; Rose, P. W. *J. Comput. Aided Mol. Des.* **2000**, *14*, 731.
- DFT calculation is performed at B3LYP/6-31G** level, with full geometry optimization in Jaguar 7.6, Schrodinger, LLC, New York, NY.